scientific reports

Check for updates

OPEN

A glucocorticoid-regulating molecule, *Fkbp5*, may interact with mitogen-activated protein kinase signaling in the organ of Corti of mice cochleae

Asuka Sato[1,3], Ryotaro Omichi[1,3], Yukihide Maeda[1,2]✉ & Mizuo Ando[1]

FKBP5 is a 51-Da FK506-binding protein and member of the immunophilin family involved in controlling the signaling of glucocorticoid receptor from the cytosol to nucleus. Fkbp5 has previously been shown to be expressed in murine cochlear tissue, including the organ of Corti (i.e., the sensory epithelium of the cochlea). *Fkbp5*$^{-/-}$ mice as used in this study show hearing loss in the low-frequency (8-kHz) range and click-evoked auditory brainstem response (ABR) threshold compared to wild-type mice. Both *Fkbp5*$^{-/-}$ and wild-type mice showed hearing loss at all frequencies and click-ABR thresholds at 24 h and 14 days following acoustic overexposure (AO). Tissues of the organ of Corti were subjected to RNA sequencing and KEGG pathway analysis. In *Fkbp5*$^{-/-}$ mice before AO, the mitogen-activated protein kinase (MAPK) signaling pathway was dysregulated compared to wild-type mice. In wild-type mice at 12 h following AO, the most significantly modulated KEGG pathway was the TNF signaling pathway and major MAPK molecules p38 and Jun were involved in the TNF signaling pathway. In *Fkbp5*$^{-/-}$ mice at 12 h following AO, the MAPK signaling pathway was dysregulated compared to wild-type mice following AO. In conclusion, *Fkbp5* interacts with MAPK signaling in the organ of Corti in mice cochleae.

Keywords The organ of Corti, Acoustic trauma, RNA sequencing, 51-Da FK506-binding protein, Mitogen-activated protein kinase signaling, Tumor necrosis factor signaling

Acute sensorineural hearing loss (ASNHL) is a frequent disease condition with limited therapeutic options in clinical practice. For example, idiopathic sudden sensorineural hearing loss (ISSNHL) affects 60.9 per 100,000 population annually in Japan[1]. Approximately two-thirds of ISSNHL patients experience a lifelong sequela of hearing loss that negatively impacts quality of life[2].

Acute inflammatory and immune reactions play major roles in pathological processes in the cochlea with ASNHL due to acoustic trauma[3], cisplatin ototoxicity[4], kanamycin ototoxicity[5] and mitochondrial dysfunction[6]. The cochlear hair cell (HC) is specialized for the unique cellular function of sound transduction, and innate immune reactions involving the organ of Corti (i.e., the cochlear sensory epithelium) provide potential therapeutic targets for ASNHL[7]. As glucocorticoids can suppress inflammatory and immune reactions in cells, many clinicians have been empirically using systemic or intratympanic glucocorticoids as therapy for ASNHL.

In the inner ear of the mouse, the potent glucocorticoid dexamethasone significantly upregulates expression of the 51-kDa FK506-binding protein (*FKBP5*) in both cultured and in vivo cochlear tissues[8,9]. FKBP5 is a member of the immunophilin molecular family and forms a protein-folding chaperone to the complex of glucocorticoid receptor (GR) and heat shock protein 90, and inhibits the signaling of GR from the cytosol to the nucleus. The *FKBP5* gene itself has multiple glucocorticoid response elements in its regulatory regions and its expression is controlled by GR, with *FKBP5* and GR forming a negative feedback loop. Generally, ligand-bound GR controls the transcription of target genes in the nucleus via the steroid signaling regulated by FKBP5[10].

[1]Department of Otolaryngology-Head and Neck Surgery, Okayama University Graduate School of Medicine, Dentistry and Pharmaceutical Sciences, 2-5-1 Shikata, Kita-Ku, Okayama 700-8558, Japan. [2]Department of Otolaryngology and Neuro-Otology, Saitama Medical University, Faculty of Medicine, Morohongo 38, Moroyamamachi, Iruma-gun, Saitama 350-0495, Japan. [3]Asuka Sato and Ryotaro Omichi have contributed equally to this work. ✉email: ymaeda@saitama-med.ac.jp

To date, several types of genetically engineered mouse models involving *FKBP5* (knockout mice, conditional knockout, overexpression and humanized mice models) have been established. In these mouse models, the functions of *Fkbp5* gene have been associated with phenotypes of neuroinflammation, hypothalamic-pituitary-adrenal (HPA) axis response, anxiety-like behavior, depressive-like behavior, learning and memory, and sleep[11]. Kwon et al. analyzed the gene transcriptome by RNA sequencing in the brain of *Fkbp5*-knockout mice exposed to chronic restraint stress[12]. That study by Kwon et al. showed that gene expressions pertaining to regulation of the immune response and the development of the neuroendocrine system were altered in *Fkbp5*-knockout mice compared to wild-type mice. Based on these concepts, the present study aimed to clarify the function of *Fkbp5* in the organ of Corti at the onset of ASNHL (acoustic trauma) by means of RNA sequencing in *Fkbp5*-knockout mice. We hypothesized that *Fkbp5* regulates immune reactions in the organ of Corti of mice cochleae with acoustic trauma.

Methods

Animals (mice)

Homozygous *Fkbp5*^{tm1Dvds}/J-knockout mice were used in this study. The breeding pair of heterozygous *Fkbp5*$^{+/-}$ mice with mixed Swiss–Webster and C57BL/6 background was purchased from Jackson Laboratory (Bar Harbor, ME). Mice were genotyped using the following PCR primers: 5′-GTTGCACCACAGATGAAACG-3′ (mutant reverse), 5′-AAAGGACAATGACTACTGATGAGG-3′ (common), and 5′-AAGGAGGGGTTCTTTTGAGG-3′ (wild-type reverse). *Fkbp5* transgenic mice show sex-dependent differences in gene expressions in neurons, body weight gain under high-fat diet treatment and stress-related behavior[13,14]. In female mice carrying a specific allele of *FKBP5*, exposure to early-life stress resulted in altered HPA axis function, exploratory behavior, and sociability[15]. Additionally, in the brains of *Fkbp5*$^{-/-}$ mice compared to wild-type mice, a greater number of differentially expressed genes were identified in female comparisons than in male comparisons[16]. With reference to these papers, female 5- to 7-week-old *Fkbp5*$^{-/-}$ mice and wild-type mice of the same sex and age were used in this study. *Fkbp5*$^{-/-}$ mice were housed under constant temperature with *ad libitum* access to food and water. Wild-type C57BL/6J mice were used as the control according to the recommendations from Jackson Laboratory (https://www.jax.org/strain/017989).

All animal experiments were performed in accordance with the ethical standards approved by the Committee on the Use and Care of Animals at Okayama University (protocol nos.: OKU-2016254, 2019021, 2022056, 2023332, 2023334, 2023465, 2023466; principal investigator: Y.M.) and performed in compliance with national and international standards of animal care and ARRIVE guidelines.

Acoustic overexposure (AO)

Awake and unrestrained mice in an anechoic chamber were exposed to 114 dB SPL octave band noise (8.0–16.0 kHz) delivered through a speaker on the top of the chamber (CF1; Tucker Davis Technologies, Gainesville, FL, USA) for 2 h. The exposure stimulus was generated and filtered with a 60-dB/octave slope by a sound generator (Rp 2.1; Tucker Davis Technologies), amplified (SA1; Tucker Davis Technologies), and delivered by the exponential speaker. Sound exposure levels were measured by a sound level meter and verified to be 114 dB SPL inside the chamber. Hearing levels of mice were assessed by auditory brainstem response (ABR) at 0 h (mice without noise), 24 h, and 14 days following AO.

Hearing function test by ABR

Mice were anesthetized by intraperitoneal injections of ketamine (80 mg/kg) and xylazine (8 mg/kg). ABRs were evoked with clicks and bursts of pure tones at frequencies of 8, 12, 16, and 32 kHz through a sound conduction tube and recorded by needle electrodes inserted through the retroauricular skin. Responses were collected using a signal processor (RA16; Tucker Davis Technologies) and BioSigRP software (Tucker Davis Technologies). Responses were processed through a 300-Hz to 5-kHz bandpass filter and averaged 500 times. Stimuli were applied in 5-dB steps from 90 dB to 5 dB SPL. ABR thresholds were defined as the lowest sound level at which the response can clearly recognized by eye from stacked waveforms. ABR thresholds between experimental groups were statistically compared using the Kruskal–Wallis test and Mann–Whitney U-test with a significance level of $P < 0.05$.

Dissection of the mouse organ of Corti and RNA extraction

Mice were anesthetized by intraperitoneal injection of ketamine (80 mg/kg) and xylazine (8 mg/kg) and killed by cervical dislocation. Tissues of the organ of Corti were dissected under a stereomicroscope (M205C; Leica, Tokyo, Japan), immersed into QIAzol Lysis reagent (QIAGEN, Tokyo, Japan), immediately frozen in liquid nitrogen and freeze-stored until RNA extraction. The dissected tissues contained both inner and outer hair cells, as well as supporting cells, as confirmed by surface preparations of the tissue specimens[17]. Tissues in the apical and middle turns were quickly dissected, typically within 10 min, because the apical and middle turns are more easily accessible under stereomicroscopy than the basal turn. Total RNA was extracted using an miRNeasy micro kit (QIAGEN). RNA integrity numbers in all RNA samples were > 7.0 as assessed using a 2100 bioanalyzer (Agilent Technologies, Tokyo, Japan). The quantity of the RNA sample was 45–420 ng in one RNA sample. Six cochlear tissues from 6 wild-type mice (one ear per mouse) were collected for one batch of the RNA sample. Eight cochlear tissues from 4 *Fkbp5*$^{-/-}$ mice (two ears per mouse) were collected for one batch of RNA sample. Biological duplicates of RNA samples were collected for each of the following experimental groups: (1) wild-type mice before AO; (2) *Fkbp5*$^{-/-}$ mice before AO; (3) wild-type mice at 12 h following AO; and (4) *Fkbp5*$^{-/-}$ mice at 12 h following AO.

RNA sequencing

Total RNA (20 ng) was subjected to purification of poly(A)-tailed mRNA using oligo-dT magnetic beads with a NEBNext Poly(A) mRNA Magnetic Isolation Module (New England Biolabs, Ipswich, MA) and the sequencing DNA library was synthesized using a NEBNext Ultra II Directional RNA Library Prep kit for Illumina (New England Biolabs). The quality of the libraries was assessed with an Agilent 2200 TapeStation High Sensitivity D1000 (Agilent Technologies). The pooled library of samples was sequenced using a 75-bp single-end on a NextSeq 500 platform (Ilumina, San Diego, CA). Sequence data of RNA transcripts were aligned using Star 2.7.10b software (GitHub, https://github.com/alexdobin/STAR) to the Mouse mm10 reference genome sequence, downloaded from the Illumina iGenomes website (http://jp.support.illumina.com/sequencing/sequencing_software/igenome.html) and annotated in reference to the Ensembl Genes database (2018.02.25) using StrandNGS 4.0 software (https://www.strand-ngs.com/). Read counts ranged from 19,400,000 to 37,100,000 in samples.

Bioinformatics analysis of differentially expressed genes (DEGs)

The mRNA transcript in the sequence data was annotated by the official gene symbols designated by the Hugo Gene Nomenclature Committee (http://www.genenames.org/). Read counts were normalized using the iDEGES method[18] and differential expression analysis was performed using edgeR software[19] to identify DEGs that were significantly up- or downregulated between samples with values of $P < 0.05$.

Biological pathways involving these DEGs were determined by Kyoto Encyclopedia of Genes and Genomes (KEGG) pathway analysis using the web-based database David Bioinformatics Resources v2023q3 (https://david.ncifcrf.gov/)[20–24]. If a subset of DEGs is found in abundance in a KEGG pathway with a value of $P < 0.05$ and a false discovery rate (FDR) < 0.05, these DEGs were deemed as significantly enriching this pathway with a specific physiological function. If a gene pathway meets both criteria—$P < 0.05$ and FDR < 0.05—it is considered to be significantly enriched.

Hierarchical clustering analysis and heatmap visualization of genes were performed using StrandNGS 4.0 software. Clustering was conducted after normalizing RNA-seq read counts with the trimmed mean of M-values method[25] and calculated using The Euclidean distance metric and Ward's linkage rule.

The protein-protein interaction (PPI) network of DEGs was then studied using the web-based STRING 12.0 analysis tool (https://string-db.org)[26]. The STRING program analyzes the mutual relationships of genes/proteins evidenced by experimentally verified interactions, co-expressions, and co-citations in curated databases and PubMed abstracts, and visualizes the gene/protein association networks. The list of DEGs was subjected to STRING and analyzed with the interaction parameters of the default setting in the program: "textmining", "experiments", "databases", "co-expression", "neighborhood", "gene-fusion", and "co-occurrence". The PPI network was visualized showing the confidence of interactions between genes/proteins with a medium confidence score of 0.4.

In silico analysis of *Fkbp5* expression in HCs

In a previous paper, an immunohistochemical experiment showed that Fkbp5 protein is expressed in cochlear HCs and supporting cells of adult mice[9]. In the present paper, expression levels of *Fkbp5* specifically in outer HCs (OHCs) and inner HCs (IHCs) were determined by exploring the data deposited in the Shared Harvard Inner Ear Laboratory Database (https//shield.hms.harvard.edu). SHIELD is a freely available database of cell type-specific gene expressions in the inner ear[27]. The data in SHIELD were generated as follows: cochleae were dissected from mice expressing eGFP under the *Pou4f3* promotor which drives HC-specific transcriptions. The spiral ganglion and Reissener's membrane were removed from the cochlear tissue, cells were dissociated in buffers, and HCs (eGFP-positive cells) and surrounding cells (eGFP-negative cells) were separately collected by fluorescence-activated cell sorting. After RNA extraction and poly-A mRNA purification, cDNA library was constructed, and gene expression levels were determined as read counts by Illumina sequencing. In experiments specifically in OHCs and IHCs, 2000 OHCs and 2000 IHCs were manually collected by suction pipette technique. Gene expression levels in OHCs and IHCs were determined using GeneChip Mouse Gene 2.0 ST arrays (Affymetrix, Santa Clare, CA).

Results

AO and hearing function test by ABR

Fkbp5$^{-/-}$ mice showed significant hearing loss compared to wild-type mice at low frequency (*Fkbp5*$^{-/-}$ at 8 kHz, 30.8 ± 4.9 dB SPL, mean ± SD, $n = 6$; wild-type at 8 kHz, 16.4 ± 6.3, $n = 7$) and with click stimuli (*Fkbp5*$^{-/-}$, 41.7 ± 4.1 dB SPL, $n = 6$; wild-type, 32.9 ± 3.9, $n = 7$) before AO ($P < 0.05$; Fig. 1C). Wild-type mice showed significant noise-induced hearing loss at 24 h (8 kHz, 58.3 ± 20.9, $n = 6$; 16 kHz, 65.8 ± 12.4, $n = 6$; 24 kHz, 75.0 ± 5.5, $n = 6$; 32 kHz, 80.8 ± 5.8, $n = 6$; click, 66.7 ± 9.8, $n = 6$) and 14 days (8 kHz, 43.3 ± 12.1, $n = 6$; 16 kHz, 50.8 ± 18.8, $n = 6$; 24 kHz, 70.8 ± 5.8, $n = 6$; 32 kHz, 76.7 ± 2.6, $n = 6$; click, 51.7 ± 6.8, $n = 6$) following AO compared to hearing levels before AO (8 kHz, 16.4 ± 6.3, $n = 7$; 16 kHz, 14.3 ± 3.5, $n = 7$; 24 kHz, 24.3 ± 3.5, $n = 7$; 32 kHz, 32.9 ± 10.4, $n = 7$; click, 32.9 ± 3.9, $n = 7$) ($P < 0.05$; Fig. 1A). *Fkbp5*$^{-/-}$ mice showed significant noise-induced hearing loss at 24 h (8 kHz, 62.5 ± 20.4, $n = 6$; 16 kHz, 64.2 ± 18.6, $n = 6$; 24 kHz, 74.2 ± 19.6, $n = 6$; 32 kHz, 80.0 ± 20.5, $n = 6$; click, 60.0 ± 13.8, $n = 6$) and 14 days (8 kHz, 49.2 ± 20.8, $n = 6$; 16 kHz, 48.3 ± 20.2, $n = 6$; 24 kHz, 62.5 ± 9.9, $n = 6$; 32 kHz, 68.3 ± 11.7, $n = 6$; click, 59.2 ± 12.4, $n = 6$) following AO compared to hearing levels before AO (8 kHz, 30.8 ± 4.9, $n = 7$; 16 kHz, 15.8 ± 5.8, $n = 7$; 24 kHz, 30.8 ± 6.6, $n = 7$; 32 kHz, 35.8 ± 12.0, $n = 7$; click, 41.7 ± 4.1, $n = 7$; $P < 0.05$) (Fig. 1B). Hearing levels did not differ between *Fkbp5*$^{-/-}$ mice and wild-type mice at all frequencies at 24 h and 14 days following AO (Fig. 1D,E).

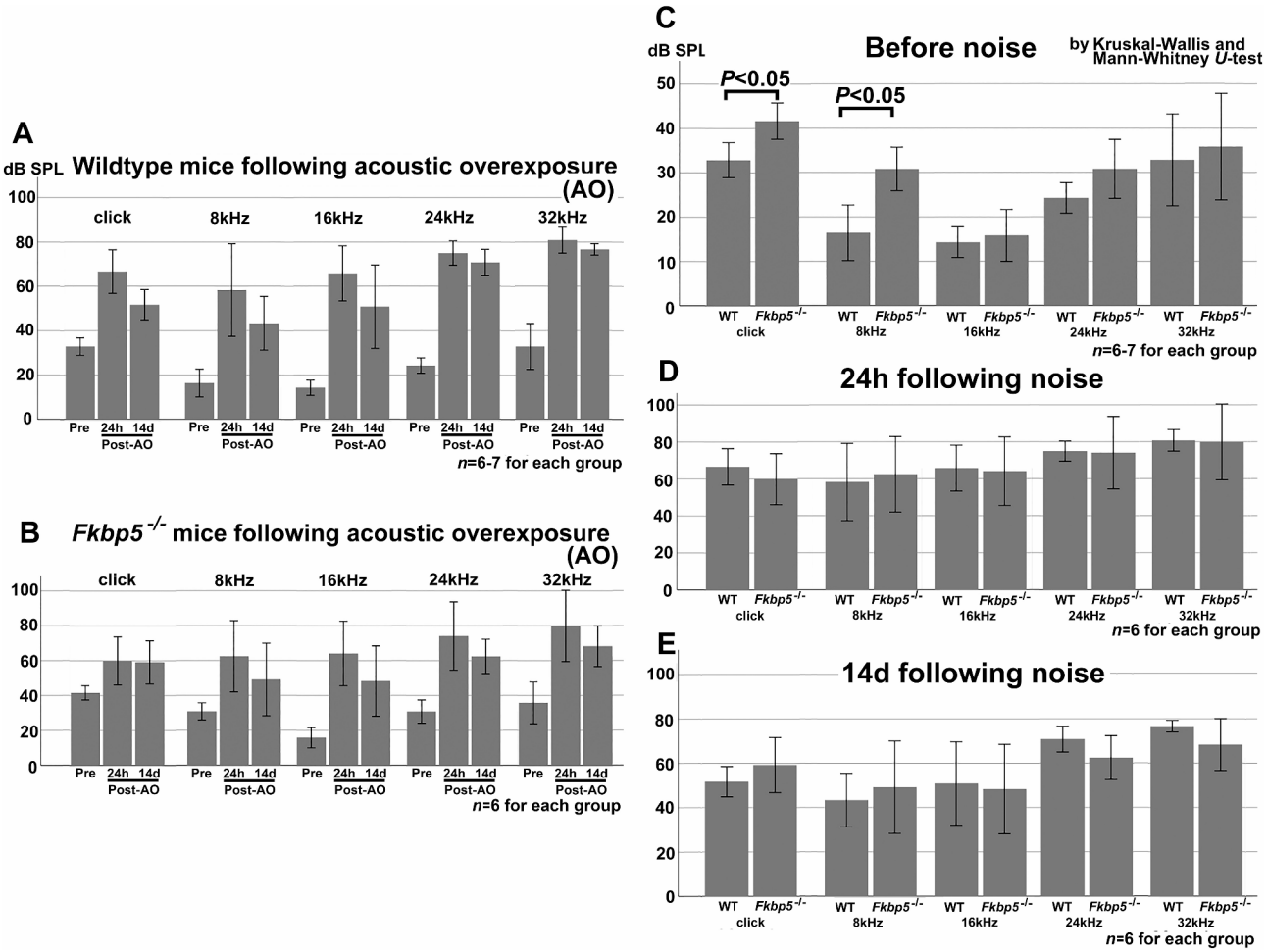

Fig. 1. Acoustic overexposure (AO) and hearing function test by auditory brainstem response (ABR). Bars represent mean (± SD) ABR thresholds. (**A**) Wild-type mice show significant noise-induced hearing loss in all frequencies at 24 h and 14 days following AO compared to hearing levels before AO. (**B**) *Fkbp5*$^{-/-}$ mice show significant noise-induced hearing loss in all frequencies at 24 h and 14 days following AO compared to hearing levels before AO. (**C**) *Fkbp5*$^{-/-}$ mice show significant hearing loss compared to wild-type mice at 8 kHz and for click stimuli before AO ($P < 0.05$). (**D**) Hearing levels do not differ between *Fkbp5*$^{-/-}$ and wild-type mice in all frequencies at 24 h following AO. (**E**) Hearing levels do not differ between *Fkbp5*$^{-/-}$ and wild-type mice in all frequencies at 14 days following AO.

Identification of DEGs in the mouse organ of Corti

Differential expression analysis using edgeR identified that expression levels of 1,426 genes were either upregulated (828 genes) or downregulated (598 genes) in the organ of Corti of wild-type mice at 12 h following AO, as compared to those of wild-type mice before AO ($P < 0.05$). In the organ of Corti in *Fkbp5*$^{-/-}$ mice before AO, 3,839 genes were either upregulated (2293 genes) or downregulated (1546) as compared to wild-type mice before AO ($P < 0.05$). In *Fkbp5*$^{-/-}$ mice at 12 h following AO, 2,651 genes were either upregulated (1343 genes) or downregulated (1308) as compared to wild-type mice at 12 h following AO ($P < 0.05$).

Bioinformatic analyses of DEGs between wild-type mice before and following AO

To gain insights into the basic molecular mechanisms in the organ of Corti with acoustic trauma, we initially analyzed the functions of DEGs comparing wild-type mice before and following AO (lower left in Table 1). In this analysis, KEGG pathways pertaining to immune reactions were predominantly modulated in wild-type mice following AO ($P < 0.05$, FDR < 0.05), such as the tumor necrosis factor (TNF) signaling pathway, the interleukin (IL)-17 signaling pathway, and cytokine-cytokine receptor interactions. The most significantly modulated KEGG pathway was the TNF signaling pathway. Modulation in steroid biosynthesis was associated with those immune reactions following AO ($P < 0.05$, FDR < 0.05). The following intracellular signaling pathways were significantly regulated following AO ($P < 0.05$, FDR < 0.05): the mitogen-activated protein kinase (MAPK) signaling pathway; the Nuclear Factor (NF)-κB signaling pathway; the p53 signaling pathway; and the phosphatidylinositol 3-kinase (PI3K)-Akt signaling pathway.

DEGs in the TNF signaling pathway included major MAPK signaling molecules p38 and Jun (i.e., c-Jun). In the molecular cascade of the TNF signaling pathway curated in the KEGG pathway database, TNF receptor

KEGG pathways modulated in Fkbp5$^{-/-}$ mice without acoustic overexposure(AO) compared to wild-type mice without AO							
KEGG pathway	**Gene count**	***P* value**	**FDR**	**KEGG pathway**	**Gene count**	***P* value**	**FDR**
MAPK signaling pathway	90	5.10E-09	4.20E-07	Ras signaling pathway	60	3.70E-04	2.00E-03
Retrograde endocannabinoid signaling	51	1.90E-07	5.30E-06	Leukocyte transendothelial migration	35	5.70E-04	2.90E-03
Glutamatergic synapse	42	2.90E-07	6.60E-06	Aldosterone synthesis and secretion	31	7.00E-04	3.20E-03
Dopaminergic synapse	46	9.40E-07	1.50E-05	Relaxin signaling pathway	35	2.60E-03	1.00E-02
Oxytocin signaling pathway	49	2.90E-06	3.60E-05	Renin secretion	23	4.20E-03	1.60E-02
Synaptic vesicle cycle	29	1.70E-05	1.60E-04	Sphingolipid signaling pathway	33	6.30E-03	2.30E-02
Circadian entrainment	34	2.00E-05	1.90E-04	Thyroid hormone synthesis	22	6.60E-03	2.40E-02
GnRH signaling pathway	31	5.90E-05	4.60E-04	cGMP-PKG signaling pathway	42	8.00E-03	2.80E-02
Wnt signaling pathway	50	6.90E-05	5.20E-04	Ferroptosis	14	9.20E-03	3.10E-02
Rap1 signaling pathway	58	8.50E-05	6.10E-04	Signaling pathways regulating pluripotency of stem cells	35	1.00E-02	3.30E-02
Hippo signaling pathway	45	1.60E-04	1.00E-03	GABAergic synapse	24	1.50E-02	4.60E-02
Cholinergic synapse	35	1.60E-04	1.00E-03	Insulin signaling pathway	34	1.60E-02	4.70E-02
PI3K-Akt signaling pathway	87	1.90E-04	1.10E-03	HIF-1 signaling pathway	29	1.60E-02	4.80E-02
Estrogen signaling pathway	39	2.80E-04	1.50E-03				
KEGG pathways modulated in wild-type mice with AO compared to wild-type mice without AO				KEGG pathways modulated in Fkbp5$^{-/-}$ mice with AO compared to wild-type mice with AO			
TNF signaling pathway	27	1.50E-08	4.20E-06	Wnt signaling pathway	39	4.30E-05	3.10E-03
IL-17 signaling pathway	22	3.70E-07	5.30E-05	Retrograde endocannabinoid signaling	33	2.10E-04	8.30E-03
Cytokine-cytokine receptor interaction	43	9.90E-07	7.10E-05	Leukocyte transendothelial migration	28	2.50E-04	8.30E-03
Steroid biosynthesis	10	1.70E-06	9.90E-05	Glutamatergic synapse	27	3.00E-04	8.60E-03
MAPK signaling pathway	39	5.70E-05	2.10E-03	Oxytocin signaling pathway	33	3.50E-04	9.10E-03
NF-kappa B signaling pathway	18	4.00E-04	1.00E-02	Circadian entrainment	24	4.20E-04	9.50E-03
p53 signaling pathway	14	7.50E-04	1.40E-02	Hippo signaling pathway	33	5.60E-04	1.10E-02
Circadian rhythm	9	1.20E-03	2.00E-02	cGMP-PKG signaling pathway	34	1.50E-03	1.90E-02
PI3K-Akt signaling pathway	40	1.30E-03	2.00E-02	GnRH signaling pathway	21	2.00E-03	2.20E-02
				MAPK signaling pathway	51	2.80E-03	2.90E-02
				Rap1 signaling pathway	38	4.90E-03	4.40E-02

Table 1. Functional gene pathways associated with differentially expressed genes (DEGs) in the organ of Corti. The biological functions of DEGs identified by edgeR software ($P < 0.05$) were significantly associated with these Kyoto Encyclopedia of Genes and Genomes (KEGG) pathways with a value of $P < 0.05$ and a false discovery rate (FDR) < 0.05.

1 (Tnfr1) was upregulated and p38 and Jun were also upregulated in the downstream cascade from TNFR1 in the mouse organ of Corti following AO (asterisks indicating DEGs in Fig. 2A). Figure 2B presents a hierarchical clustering analysis and heat map of genes in the TNF signaling pathway.

The STRING program visualized the mutual relationships of DEGs in TNF signaling pathway and Jun and IL1B genes were recognized as playing major functions in the PPI network following AO (Fig. 3). IL1B was upregulated following AO.

Bioinformatic analyses of DEGs between *Fkbp5*$^{-/-}$ and wild-type mice before AO

Next, we analyzed the functions of DEGs comparing *Fkbp5*$^{-/-}$ mice before AO and wild-type mice before AO (upper part in Table 1). MAPK signaling was one of the top three most significantly dysregulated KEGG pathways in *Fkbp5*$^{-/-}$ mice. The following KEGG pathways pertaining to intracellular signaling were dysregulated in *Fkbp5*$^{-/-}$ mice ($P < 0.05$, FDR < 0.05): MAPK signaling pathway, oxytocin signaling pathway, GnRH signaling pathway, Wnt signaling pathway, Rap1 signaling pathway, Hippo signaling pathway, PI3K-Akt signaling pathway, estrogen signaling pathway, Ras signaling pathway, relaxin signaling pathway, sphingolipid signaling pathway, cGMP-PKG signaling pathway, insulin signaling pathway and HIF-1 signaling pathway. The following KEGG pathways pertaining to synaptic transmission were also dysregulated in *Fkbp5*$^{-/-}$ mice ($P < 0.05$, FDR < 0.05): retrograde endocannabinoid signaling, glutamatergic synapses, dopaminergic synapses, synaptic vesicle cycle, cholinergic synapses and GABAergic synapse. Other dysregulated KEGG pathways include "ferroptosis" and "signaling pathways regulating pluripotency of stem cells" ($P < 0.05$, FDR < 0.05).

In the molecular cascade of MAPK signaling curated in the KEGG pathway database, all classical MAPK pathways (i.e., extracellular signal-regulated kinases [ERK] MAPK pathway, c-Jun N-terminal kinases [JNK] MAPK pathway, and p38 MAPK pathways) were dysregulated in *Fkbp5*$^{-/-}$ mice (asterisks in Fig. 4A). Jun and p38 were both upregulated in *Fkbp5*$^{-/-}$ mice before AO. Figure 4B presents a hierarchical clustering analysis and heat map of genes in the MAPK signaling pathway in wild-type and *Fkbp5*$^{-/-}$ mice before AO.

The STRING program visualized the mutual relationships of DEGs in the MAPK signaling pathway and Jun and p38 were recognized as playing a major function in the PPI network in *Fkbp5*$^{-/-}$ mice before AO (Fig. 5).

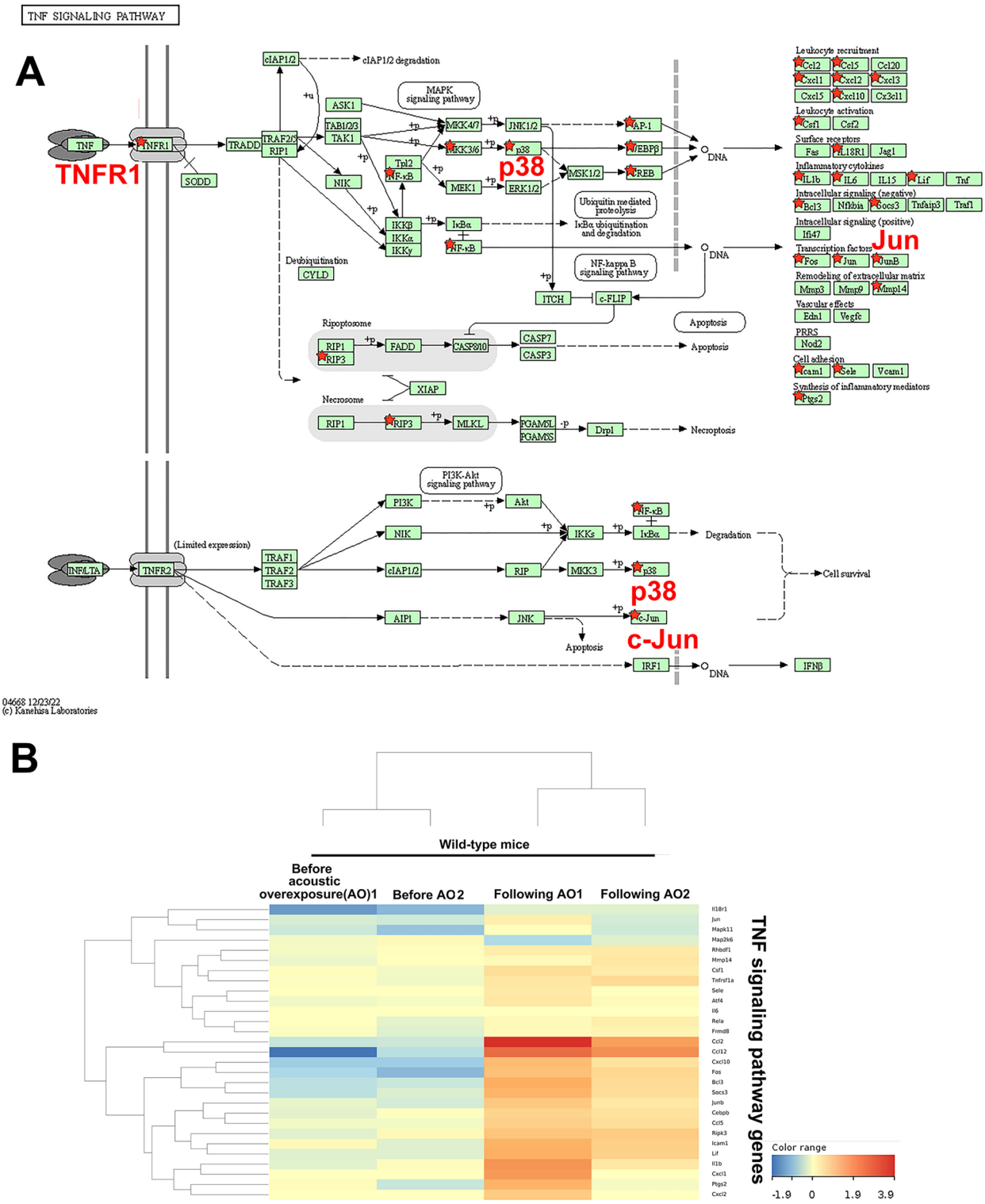

Fig. 2. Tumor necrosis factor signaling pathway regulated in the organ of Corti in wild-type mice following acoustic overexposure (AO). (**A**) TNF signaling pathway curated in the database of Kyoto Encyclopedia of Genes and Genomes (KEGG). Asterisks show differentially regulated genes in wild-type mice following AO as compared to wild-type mice before AO. The figure is reprinted with the permission of KEGG. (**B**) A hierarchical clustering analysis and heat map of genes in the TNF signaling pathway. The color gradient from blue to red represents low to high gene expression levels. Each row corresponds to the expression level of a specific gene, while each column represents RNA samples from wild-type mice before and after AO.

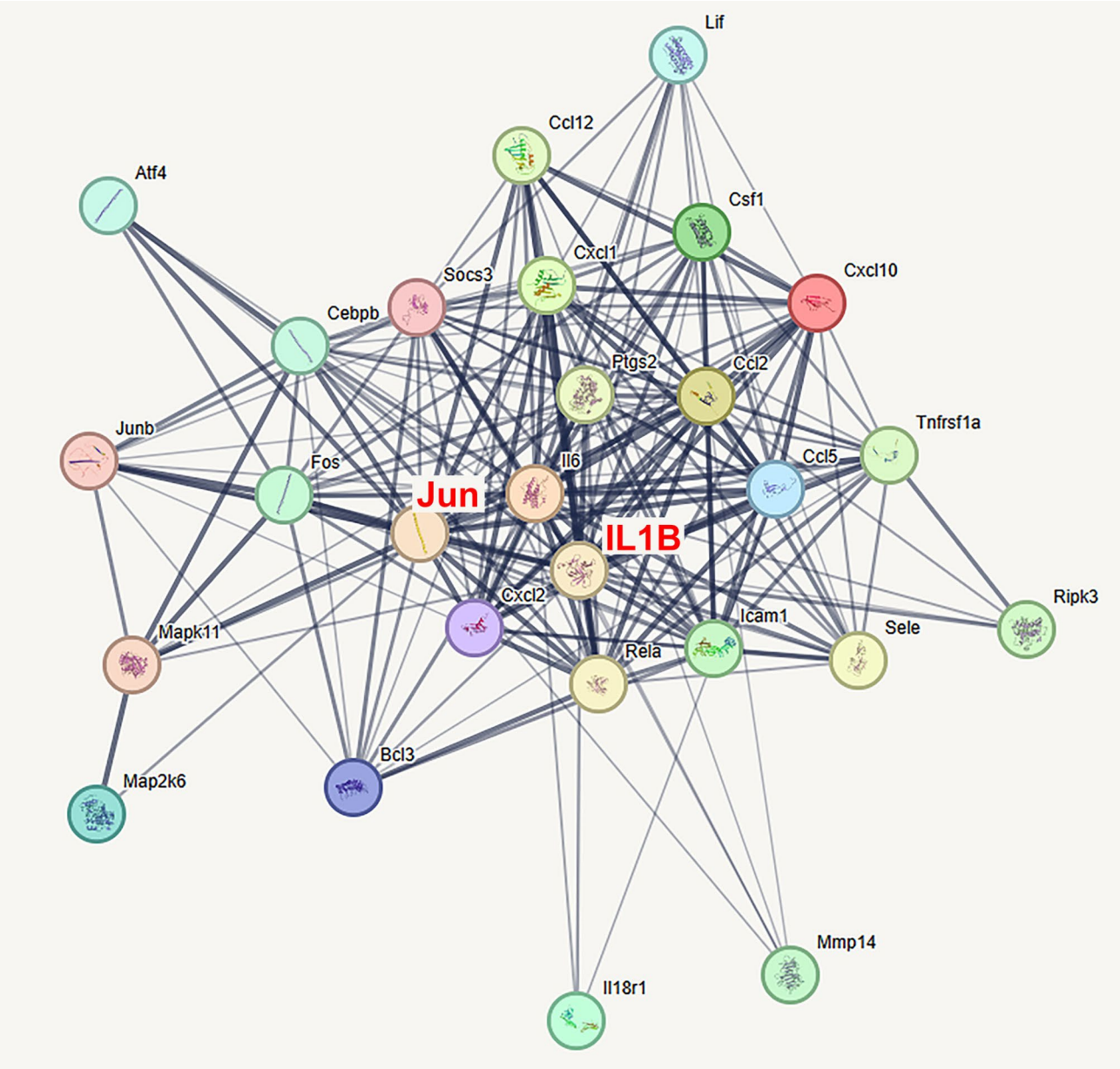

Fig. 3. Association network of differentially expressed genes (DEGs) in the tumor necrosis factor signaling pathway in the organ of Corti in wild-type mice following acoustic overexposure (AO). The network of DEGs in the TNF pathway in wild-type mice following AO as compared to wild-type mice before AO. Jun and IL1B are recognized as key regulators in the protein-protein interaction network of the TNF signaling pathway following AO. The STRING database (https://string-db.org) computed the graphical analysis of mutual relationships of the DEGs as evidenced by experimentally verified interactions, co-expressions, and co-citations in curated databases and PubMed abstracts. The figure downloaded from STRING is freely available under a 'Creative Commons BY 4.0' license (https://creativecommons.org/licences/by/4.0/).

Bioinformatic analyses of DEGs between *Fkbp5*$^{-/-}$ and wild-type mice following AO

We further analyzed the functions of DEGs comparing *Fkbp5*$^{-/-}$ mice following AO and wild-type mice following AO (lower right in Table 1). The following KEGG pathways pertaining to intracellular signaling were dysregulated in *Fkbp5*$^{-/-}$ mice ($P < 0.05$, FDR < 0.05): Wnt signaling pathway, oxytocin signaling pathway, Hippo signaling pathway, cGMP-PKG signaling pathway, GnRH signaling pathway, MAPK signaling pathway, and Rap1 signaling pathway. KEGG pathways pertaining to synaptic transmission were also dysregulated in *Fkbp5*$^{-/-}$ mice ($P < 0.05$, FDR < 0.05): retrograde endocannabinoid signaling, and glutamatergic synapses.

The STRING program visualized the mutual relationships of DEGs in the MAPK signaling pathway. Major proinflammatory cytokines, TNF and IL1B were downregulated in the MAPK signaling pathway in *Fkbp5*$^{-/-}$ mice following AO. These proinflammatory cytokines play important functions in the PPI network of DEGs of MAPK signaling dysregulated in *Fkbp5*$^{-/-}$ mice following AO (Fig. 6).

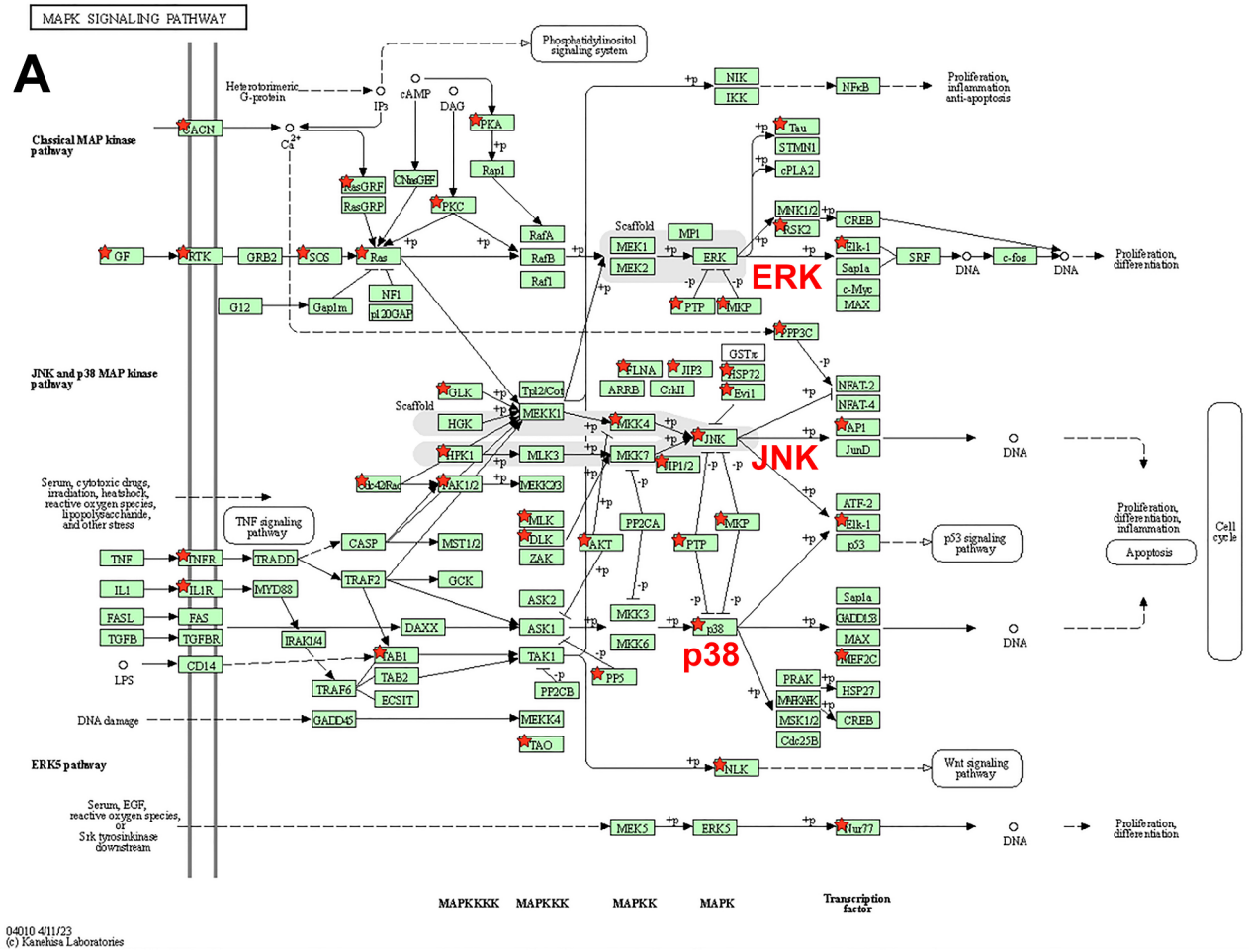

Fig. 4. MAPK signaling pathway regulated in the organ of Corti in *Fkbp5*$^{-/-}$ mice before acoustic overexposure (AO). (**A**) MAPK signaling pathway curated in the database of the Kyoto Encyclopedia of Genes and Genomes (KEGG). Asterisks show differentially regulated genes in *Fkbp5*$^{-/-}$ mice before AO as compared to wild-type mice before AO. This figure is reprinted with the permission of KEGG. (**B**) A hierarchical clustering analysis and heat map of genes in the MAPK signaling pathway. The color gradient from blue to red represents low to high gene expression levels. Each row corresponds to the expression level of a specific gene, while each column represents RNA samples from wild-type and *Fkbp5*$^{-/-}$ mice before AO.

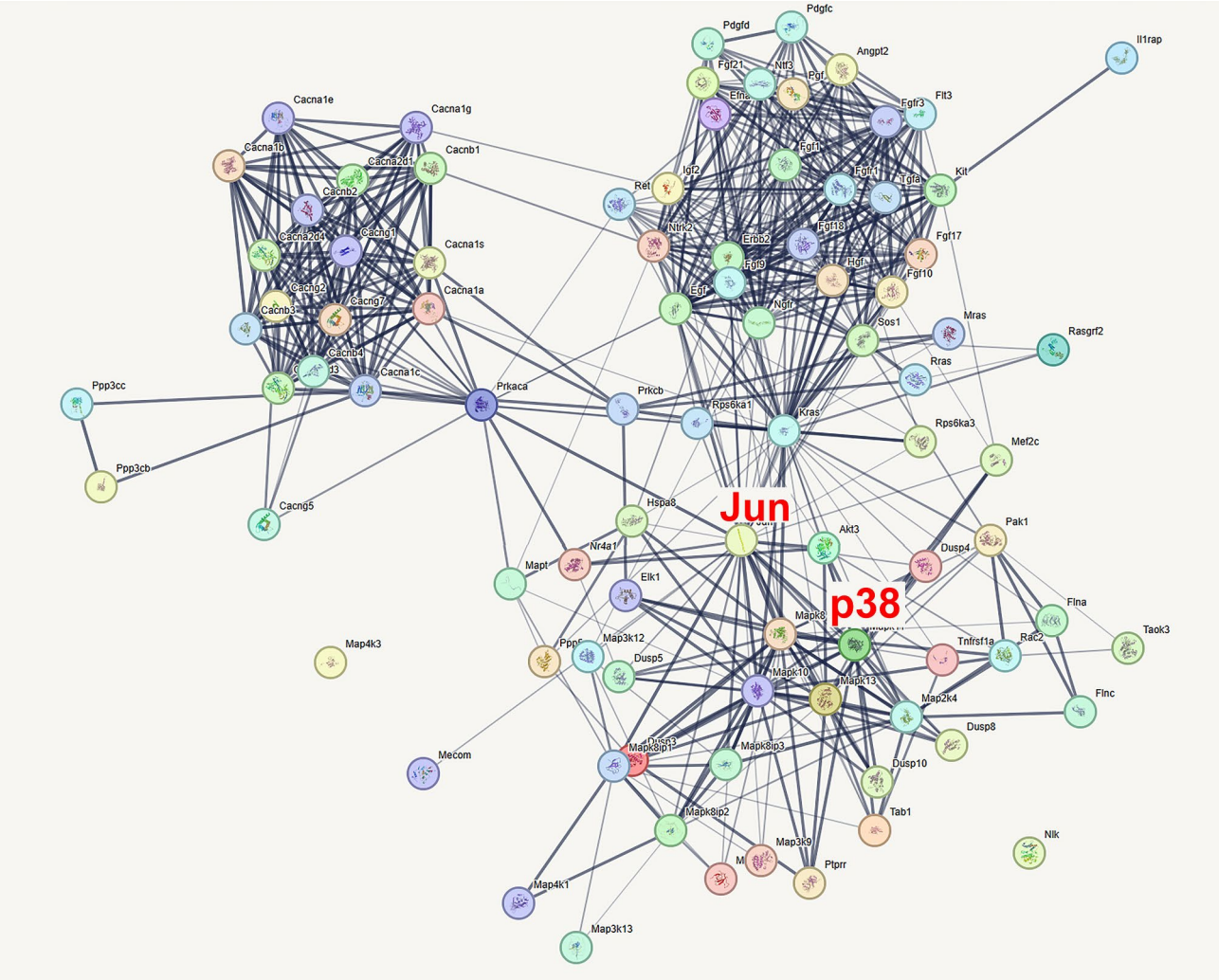

Fig. 5. Association network of differentially expressed genes (DEGs) in the MAPK pathway in the organ of Corti in *Fkbp5*$^{-/-}$ mice before acoustic overexposure (AO). The network of DEGs in the MAPK pathway in *Fkbp5*$^{-/-}$ mice before AO as compared to wild-type mice before AO. Jun and p38 are recognized as key regulators in the protein-protein interaction network of MAPK signaling in *Fkbp5*$^{-/-}$ mice before AO. The STRING database (https://string-db.org) computed the graphical analysis of mutual relationships of DEGs as evidenced by experimentally verified interactions, co-expressions, and co-citations in curated databases and PubMed abstracts. The figure downloaded from STRING is freely available under a 'Creative Commons BY 4.0' license (https://creativecommons.org/licences/by/4.0/).

In silico analysis of *Fkbp5* expression in HCs

In the dataset of RNAseq deposited in SHIELD, 18,199 genes among 20,207 annotated genes were expressed in HCs and surrounding cells with read counts ≥15[28]. Read counts of *Fkbp5* expression were 54 and 16, respectively, in HCs and surrounding cells on postnatal day 7. With these data, the *Fkbp5* read count in HCs was more than 2-fold higher than those in surrounding cells. *Fkbp5* expression levels in OHCs and IHCs were 7.13 ± 1.19 and 6.48 ± 0.17 (mean ± SD, 1.10-fold change; FDR, 0.715) in adult mice on postnatal day 25–30. Overall, *Fkbp5* may be expressed at higher levels in HCs than in other types of cochlear cells, and expressed at similar levels in OHCs and IHCs.

Discussion

According to the present data, *Fkbp5*$^{-/-}$ mice showed significant hearing loss in the low-frequency range. *Fkbp5* may thus play important roles in hearing. Hearing levels in *Fkbp5*$^{-/-}$ mice were not different from those of wild-type mice following AO. This may be because the AO in our experiment (114 dB SPL for 2 h) induced such large changes and variations in hearing levels that differences in levels between *Fkbp5*$^{-/-}$ and wild-type mice could not be detected following AO.

Fkbp5$^{-/-}$mice exhibited poorer hearing thresholds in the low-frequency range compared to wild-type mice before AO, but these differences disappeared following AO. These results could suggest that KO mice experienced less noise-induced hearing loss.

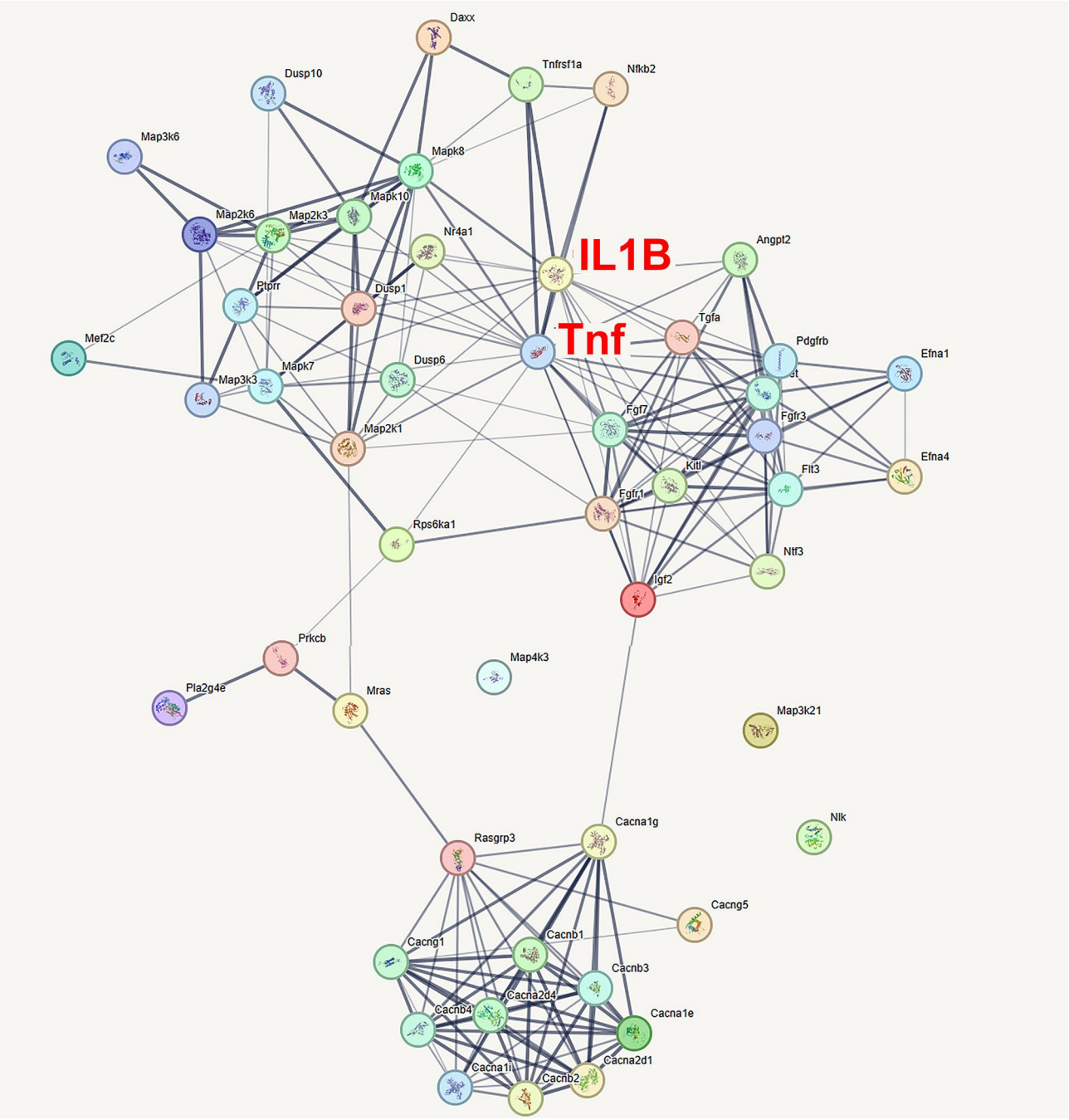

Fig. 6. Association network of differentially expressed genes (DEGs) in the MAPK pathway in the organ of Corti in *Fkbp5*$^{-/-}$ mice following acoustic overexposure (AO). The network of DEGs in the MAPK pathway in *Fkbp5*$^{-/-}$ mice following AO as compared to wild-type mice following AO. The major proinflammatory cytokines, TNF and IL1B, are recognized as key regulators in the protein-protein interaction network of MAPK signaling in *Fkbp5*$^{-/-}$ mice following AO. The STRING database (https://string-db.org) computed the graphical analysis of the mutual relationships of DEGs as evidenced by experimentally verified interactions, co-expressions, and co-citations in curated databases and PubMed abstracts. The figure downloaded from STRING is freely available under a 'Creative Commons BY 4.0' license (https://creativecommons.org/licences/by/4.0/).

Previously published immunohistochemical analyses showed that Fkbp5 is expressed in OHCs, IHCs, and supporting cells in the organ of Corti in the mouse cochlea[9]. To corroborate this, in silico analysis showed that *Fkbp5* is expressed in the organ of Corti at similar levels in OHCs and IHCs.

In our data from wild-type mice, immune reaction was the major molecular function activated in the organ of Corti at 12 h after AO. The TNF inflammatory cytokine signaling pathway was the most significantly modulated

gene expression pathway in wild-type mice following AO. This observation agrees with a previously published paper showing immune defense as the primary function associated with DEGs in the cochlea following acoustic trauma[29]. Glucocorticoids may play important roles in these immune reactions, as suggested by our data that the steroid biosynthesis pathway was significantly modulated in the organ of Corti following AO.

The MAPK signaling pathway was the most significantly changed intracellular signaling pathway in the cochleae of wild-type mice following AO. In general, the MAPK signaling pathway controls cellular responses to diverse types of extracellular stimuli such as proinflammatory cytokines, heat shock, and AO affecting the sensory organ of the cochlea[30]. MAPK signaling pathways comprise the classical MAPK pathway (i.e., ERK MAPK pathway), JNK MAPK pathway (i.e., c-Jun N-terminal kinase pathway), and p38 MAPK pathway. These three types of major MAPK pathways regulate gene expression, cell survival and apoptosis, proliferation and mitosis, and differentiation[31]. In our bioinformatics analyses, MAPK signaling by *Jun* and *p38* may be upregulated in the downstream cascade of the TNF signaling pathway in the organ of Corti following AO. *Jun* was a primary component of the network for the immune gene expression of the TNF signaling pathway. These MAPK signaling pathways may also induce a secondary immune reaction by increasing expressions of several inflammatory cytokines, including TNF[32]. MAPK signaling pathways may therefore function in both up- and downstream cascades of the TNF signaling pathway. In our dataset, the NF-κB signaling pathway was found to be significantly changed in the organ of Corti following AO. In general, the p38 MAPK pathway regulates the NF-κB signaling pathway. NF-κB is a primary transcription factor that controls the expression of *TNF* mRNA.

In *Fkbp5*$^{-/-}$ mice before AO, the three major MAPK pathways were dysregulated as compared to wild-type mice. Fkbp5 is a molecular chaperone that regulates the folding and conformation of GR and inhibits the action of GR[10]. Previous studies have indicated that MAPK signaling is overactivated in cells that have developed glucocorticoid resistance due to long-term glucocorticoid treatment among patients with asthma or chronic obstructive pulmonary disease[33]. Similarly, in the organ of Corti of *Fkbp5*$^{-/-}$ mice, GR signaling may be overactivated and Jun and P38 were upregulated.

In the presence of acoustic trauma following AO, the MAPK signaling pathway was dysregulated in *Fkbp5*$^{-/-}$ mice as compared to wild-type mice. This MAPK dysregulation in the organ of Corti is thought to be associated with the changes in immune reactions. Supporting this idea, the major proinflammatory cytokines TNF and IL1B were downregulated in the gene expression network of the dysregulated MAPK pathway in the organ of Corti following AO. In previously published data, the ligand-bound GR negatively interferes with MAPK signaling pathways and exerts anti-inflammatory effects in cells stimulated by proinflammatory or extracellular stress[34].

Previously, Meltser et al. performed experiments in which mice were restrained in a 50-ml plastic tube and exposed to AO[35]. The restraint stress (RS) activates the hypothalamic-pituitary-adrenal axis and increases plasma glucocorticoid levels. In data accumulated by Meltser et al., ERK was downregulated in the organ of Corti and the cochlear lateral wall after RS and AO, while p38 was upregulated in the auditory nerve after RS. These changes in the MAPK pathway in cochleae were attenuated by injections of glucocorticoid-antagonists to mice. Endogenous GR signaling was temporarily upregulated by RS in the experiment of Meltser et al., whereas endogenous GR signaling may have been overactivated for long periods by the loss of *Fkbp5* in our knockout mice.

Animal experiments have demonstrated that glucocorticoids effectively protect the hearing function from ASNHL caused by noise exposure[36,37], ischemia[38], and ototoxic drugs[39–41]. As a conclusion from the present study, the MAPK signaling pathway regulates cellular responses to AO and plays a critical role in the sensory function of the cochlea. In the organ of Corti of our *Fkbp5*$^{-/-}$ mice, both before and after AO, the three major MAPK pathways exhibited dysregulation compared to wild-type mice. Previous mechanistic studies in cellular models have demonstrated functional interactions between the glucocorticoid receptor and MAPK signaling pathways[33,34]. Therefore, A glucocorticoid-regulating molecule, *Fkbp5*, may interact with MAPK signaling in the organ of Corti of mice cochleae.

In addition, *Fkbp5*$^{-/-}$ mice showed dysregulation of gene expressions pertaining to synaptic neurotransmission[13]. Both excitatory synapses (glutamatergic synapses) and inhibitory synapses (GABAergic synapses) were dysregulated in the organ of Corti in our *Fkbp5*$^{-/-}$ mice. This is particularly important given that the current study used female mice. A recent study reported that synaptic transmission-related genes exhibit female-biased expression[42]. This suggests that *Fkbp5* gene knockout may preferentially influence female synaptic transmission, potentially explaining the sex-dependent effects of *Fkbp5* on neural function.

Limitations of the study

In the differential gene expression analysis conducted in this study, significance was determined using raw *P*-values without applying FDR correction. This relatively low-stringency approach was adopted because the primary objective was to perform exploratory expression profiling aimed at identifying significantly regulated gene pathways—pathways characterized by the concerted behavior of multiple DEGs[43]. Although the data allowed for the identification of these gene pathways, it should be noted that the results for individual DEGs may be susceptible to false-positive findings. In future studies, it is warranted to conduct qRT-PCR or Western blotting to validate key DEGs, particularly those associated with the MAPK and TNF signaling pathways.

Fkbp5$^{-/-}$ mice were generated on a mixed genetic background of C57BL/6 and Swiss-Webster strains, and C57BL/6J mice were used as controls in accordance with the manufacturer's recommendation. The genetic background differences between the knockout and control mice may introduce potential background effects.

Data availability

Raw RNA sequence data were deposited in the NCBI Sequence Read Archive (http://www.ncbi.nlm.nih.gov/sra) and are available through the accession number PRJNA1063481.

Received: 3 January 2025; Accepted: 27 February 2025
Published online: 03 March 2025

References

1. Nakashima, T. et al. Idiopathic sudden sensorineural hearing loss in Japan. *Acta Otolaryngol.* **134**, 1158–1163. https://doi.org/10.3109/00016489.2014.919406 (2014).
2. Härkönen, K., Kivekäs, I., Rautiainen, M., Kotti, V. & Vasama, J. P. Quality of life and hearing eight years after sudden sensorineural hearing loss. *Laryngoscope* **127**, 927–931. https://doi.org/10.1002/lary.26133 (2017).
3. Maeda, Y. et al. Targeted PCR array analysis of genes in innate immunity and glucocorticoid signaling pathways in mice cochleae following acoustic trauma. *Otol. Neurotol.* **39**, e593–e600. https://doi.org/10.1097/MAO.0000000000001874 (2018).
4. Zhang, N., Cai, J., Xu, L., Wang, H. & Liu, W. Cisplatin-induced stria vascularis damage is associated with inflammation and fibrosis. *Neural Plast.* **2020**, 8851525. https://doi.org/10.1155/2020/8851525 (2020).
5. Shimada, M. D. et al. Macrophage depletion attenuates degeneration of spiral ganglion neurons in kanamycin-induced unilateral hearing loss model. *Sci. Rep.* **13**, 16741. https://doi.org/10.1038/s41598-023-43927-9 (2023).
6. Fujioka, M. et al. Pharmacological Inhibition of cochlear mitochondrial respiratory chain induces secondary inflammation in the lateral wall: A potential therapeutic target for sensorineural hearing loss. *PLoS ONE* **9**, e90089. https://doi.org/10.1371/journal.pone.0090089 (2014).
7. Chen, D. et al. Sox2 overexpression alleviates noise-induced hearing loss by inhibiting inflammation-related hair cell apoptosis. *J. Neuroinflamm.* **19**, 59. https://doi.org/10.1186/s12974-022-02414-0 (2022).
8. Maeda, Y. et al. Microarray analysis of the effect of dexamethasone on murine cochlear explants. *Acta Otolaryngol.* **130**, 1329–1334. https://doi.org/10.3109/00016489.2010.498836 (2010).
9. Maeda, Y., Fukushima, K., Kariya, S., Orita, Y. & Nishizaki, K. Intratympanic dexamethasone up-regulates Fkbp5 in the cochleae of mice in vivo. *Acta Otolaryngol.* **132**, 4–9. https://doi.org/10.3109/00016489.2011.619571 (2012).
10. Fries, G. R., Gassen, N. C. & Rein, T. The FKBP51 glucocorticoid receptor co-chaperone: Regulation, function, and implications in health and disease. *Int. J. Mol. Sci.* **18**. https://doi.org/10.3390/ijms18122614 (2017).
11. Gebru, N. T., Hill, S. E. & Blair, L. J. Genetically engineered mouse models of FK506-binding protein 5. *J. Cell. Biochem.* https://doi.org/10.1002/jcb.30374 (2023).
12. Kwon, J., Kim, Y. J., Choi, K., Seol, S. & Kang, H. J. Identification of stress resilience module by weighted gene co-expression network analysis in Fkbp5-deficient mice. *Mol. Brain* **12**, 99. https://doi.org/10.1186/s13041-019-0521-9 (2019).
13. van Doeselaar, L. et al. Sex-specific and opposed effects of FKBP51 in glutamatergic and GABAergic neurons: Implications for stress susceptibility and resilience. *Proc. Natl. Acad. Sci. U S A* **120**, e2300722120. https://doi.org/10.1073/pnas.2300722120 (2023).
14. Wang, L. et al. FKBP51-Hsp90 interaction-deficient mice exhibit altered endocrine stress response and sex differences under high-fat diet. *Mol. Neurobiol.* https://doi.org/10.1007/s12035-023-03627-x (2023).
15. Nold, V. et al. Impact of Fkbp5 X early life adversity X sex in humanised mice on multidimensional stress responses and circadian rhythmicity. *Mol. Psychiatry.* **27**, 3544–3555. https://doi.org/10.1038/s41380-022-01549-z (2022).
16. Williams, K. E. et al. Sex-specific impact of Fkbp5 on hippocampal response to acute alcohol injection: Involvement in alterations of metabolism-related pathways. *Cells* **13**. https://doi.org/10.3390/cells13010089 (2023).
17. Omichi, R., Yoshimura, H., Shibata, S. B., Vandenberghe, L. H. & Smith, R. J. H. Hair cell transduction efficiency of single- and dual-AAV serotypes in adult murine cochleae. *Mol. Ther. Methods Clin. Dev.* **17**, 1167–1177. https://doi.org/10.1016/j.omtm.2020.05.007 (2020).
18. Sun, J., Nishiyama, T., Shimizu, K. & Kadota, K. TCC: An R package for comparing tag count data with robust normalization strategies. *BMC Bioinform.* **14**, 219. https://doi.org/10.1186/1471-2105-14-219 (2013).
19. Robinson, M. D., McCarthy, D. J. & Smyth, G. K. EdgeR: A bioconductor package for differential expression analysis of digital gene expression data. *Bioinformatics* **26**, 139–140. https://doi.org/10.1093/bioinformatics/btp616 (2010).
20. Huang da, W., Sherman, B. T. & Lempicki, R. A. Systematic and integrative analysis of large gene lists using DAVID bioinformatics resources. *Nat. Protoc.* **4**, 44–57. https://doi.org/10.1038/nprot.2008.211 (2009).
21. Huang da, W., Sherman, B. T. & Lempicki, R. A. Bioinformatics enrichment tools: Paths toward the comprehensive functional analysis of large gene lists. *Nucleic Acids Res.* **37**, 1–13. https://doi.org/10.1093/nar/gkn923 (2009).
22. Kanehisa, M. Toward understanding the origin and evolution of cellular organisms. *Protein Sci.* **28**, 1947–1951. https://doi.org/10.1002/pro.3715 (2019).
23. Kanehisa, M. & Goto, S. KEGG: Kyoto encyclopedia of genes and genomes. *Nucleic Acids Res.* **28**, 27–30. https://doi.org/10.1093/nar/28.1.27 (2000).
24. Kanehisa, M., Furumichi, M., Sato, Y., Matsuura, Y. & Ishiguro-Watanabe, M. KEGG: Biological systems database as a model of the real world. *Nucleic Acids Res.* **53**, D672–D677. https://doi.org/10.1093/nar/gkae909 (2025).
25. Robinson, M. D. & Oshlack, A. A scaling normalization method for differential expression analysis of RNA-seq data. *Genome Biol.* **11**, R25. https://doi.org/10.1186/gb-2010-11-3-r25 (2010).
26. Szklarczyk, D. et al. STRING v11: Protein-protein association networks with increased coverage, supporting functional discovery in genome-wide experimental datasets. *Nucleic Acids Res.* **47**, D607–D613. https://doi.org/10.1093/nar/gky1131 (2019).
27. Shen, J., Scheffer, D. I., Kwan, K. Y. & Corey, D. P. SHIELD: An integrative gene expression database for inner ear research. Database (Oxford) 2015. https://doi.org/10.1093/database/bav071 (2015).
28. Scheffer, D. I., Shen, J., Corey, D. P. & Chen, Z. Y. Gene expression by mouse inner ear hair cells during development. *J. Neurosci.* **35**, 6366–6380. https://doi.org/10.1523/JNEUROSCI.5126-14.2015 (2015).
29. Yang, S. et al. Immune defense is the primary function associated with the differentially expressed genes in the cochlea following acoustic trauma. *Hear. Res.* **333**, 283–294. https://doi.org/10.1016/j.heares.2015.10.010 (2016).
30. Maeda, Y., Fukushima, K., Omichi, R., Kariya, S. & Nishizaki, K. Time courses of changes in phospho- and total-MAP kinases in the cochlea after intense noise exposure. *PLoS ONE* **8**, e58775. https://doi.org/10.1371/journal.pone.0058775 (2013).
31. Pearson, G. et al. Mitogen-activated protein (MAP) kinase pathways: Regulation and physiological functions. *Endocr. Rev.* **22**, 153–183. https://doi.org/10.1210/edrv.22.2.0428 (2001).
32. Sabio, G. & Davis, R. J. TNF and MAP kinase signalling pathways. *Semin Immunol.* **26**, 237–245. https://doi.org/10.1016/j.smim.2014.02.009 (2014).
33. Sevilla, L. M. et al. Glucocorticoid resistance: Interference between the glucocorticoid receptor and the MAPK signalling pathways. *Int. J. Mol. Sci.* **22**. https://doi.org/10.3390/ijms221810049 (2021).
34. Ayroldi, E. et al. Mechanisms of the anti-inflammatory effects of glucocorticoids: Genomic and nongenomic interference with MAPK signaling pathways. *FASEB J.* **26**, 4805–4820. https://doi.org/10.1096/fj.12-216382 (2012).
35. Meltser, I., Tahera, Y. & Canlon, B. Glucocorticoid receptor and mitogen-activated protein kinase activity after restraint stress and acoustic trauma. *J. Neurotrauma.* **26**, 1835–1845. https://doi.org/10.1089/neu.2008.0874 (2009).
36. Han, M. A. et al. Therapeutic effect of dexamethasone for noise-induced hearing loss: Systemic versus intratympanic injection in mice. *Otol. Neurotol.* **36**, 755–762. https://doi.org/10.1097/MAO.0000000000000759 (2015).
37. Tabuchi, K. et al. Therapeutic time window of Methylprednisolone in acoustic injury. *Otol. Neurotol.* **27**, 1176–1179. https://doi.org/10.1097/01.mao.0000226313.82069.3f (2006).

38. Morawski, K., Telischi, F. F., Bohorquez, J. & Niemczyk, K. Preventing hearing damage using topical dexamethasone during reversible cochlear ischemia: An animal model. *Otol. Neurotol.* **30**, 851–857. https://doi.org/10.1097/MAO.0b013e3181b12296 (2009).
39. Himeno, C. et al. Intra-cochlear administration of dexamethasone attenuates aminoglycoside ototoxicity in the guinea pig. *Hear. Res.* **167**, 61–70. https://doi.org/10.1016/s0378-5955(02)00345-3 (2002).
40. Daldal, A., Odabasi, O. & Serbetcioglu, B. The protective effect of intratympanic dexamethasone on cisplatin-induced ototoxicity in guinea pigs. *Otolaryngol. Head Neck Surg.* **137**, 747–752. https://doi.org/10.1016/j.otohns.2007.05.068 (2007).
41. Park, Y. S., Jung, T. T., Choi, D. J. & Rhee, C. K. Effect of corticosteroid treatment on salicylate ototoxicity. *Ann. Otol. Rhinol. Laryngol.* **103**, 896–900. https://doi.org/10.1177/000348949410301112 (1994).
42. Ye, M., Marzullo, B., Adler, H. J. & Hu, B. H. Expression profiling of cochlear genes uncovers sex-based cellular function in mouse cochleae. *Hear. Res.* **448**, 109030. https://doi.org/10.1016/j.heares.2024.109030 (2024).
43. Sadeghi, Z. et al. Transcriptomic analysis of human mesenchymal stem cell therapy in incontinent rat injured urethra. *Tissue Eng. Part. A.* **26**, 792–810. https://doi.org/10.1089/ten.tea.2020.0033 (2020).

Acknowledgements

This work was supported by JSPS KAKENHI Grant Nos. JP16K20248 (principal investigator: R.O.), JP19K09845 (Y.M.), JP22K09744 (Y.M.) and JP24K12696 (R.O.). The Japan Society for the Promotion of Science played no roles in the study design; in the collection, analysis or interpretation of data; in the writing of the report; or in the decision to submit the article for publication. Authors Asuka Sato and Ryotaro Omichi contributed equally to this work.

Author contributions

R.O.,Y.M. designed the research; A.S., R.O., Y.M. performed physiological and anatomical experiments; Y.M. analyzed data; Y.M. wrote the original draft; A.S., R.O.,Y.M., M.A. reviewed and edited the manuscript; R.O.,Y.M. acquired the funding; R.O.,Y.M, M.A. provided the resources; Y.M., M.A., supervised the research.

Declarations

Competing interests

The authors declare no competing interests.

Additional information

Correspondence and requests for materials should be addressed to Y.M.

Reprints and permissions information is available at www.nature.com/reprints.

Publisher's note Springer Nature remains neutral with regard to jurisdictional claims in published maps and institutional affiliations.